



MODELING THE STRENGTH-TO-MASS RATIO OF THE FUSED FILAMENT FABRICATED ABS POLYMER WITH ANN

Anastasios Tzotzis¹, Athanasios Manavis², Nikolaos Efkolidis³, Panagiotis Kyratsis⁴

¹⁻⁴University of Western Macedonia, Department of Product and Systems Design Engineering, 50100 Kila Kozani, Greece

Corresponding author: Panagiotis Kyratsis, pkyratsis@uowm.gr

Abstract: The present study investigated the Strength-to-Mass ratio (StMr) yielded by Acrylonitrile Butadiene Styrene (ABS) specimens, fabricated with the Fused Filament Fabrication (FFF) method. A universal testing machine was utilized for the Ultimate-Tensile-Strength (UTS) measurement of the specimens, whereas a precision balance was used to measure their mass. The experiments were designed according to the Central-Composite-Design (CCD), by considering four process parameters: the infill, the layer thickness, the line direction of the top and bottom layers, as well as the pattern. In addition, a shallow Artificial Neural Network (ANN) was developed to predict the StMr, which was then compared to the empirical model generated by the CCD method. The analysis revealed a strong correlation between the two models, with the Mean Absolute Percentage Error (MAPE) being below 1%. Finally, verification testing was performed to evaluate the absolute error handling of the ANN model, which was found to be <6%.

Key words: 3D printing; ABS; Artificial neural network; Central composite design; Fused Deposition Modeling; Strength to mass ratio.

1. INTRODUCTION

Fused Filament Fabrication (FFF) is one of the latest manufacturing processes available in the industry, being used for modelling, prototyping and production applications. By having advantages such as the ability to produce strong and at the same time lightweight parts, as well as the fact that it is one of the most environmentally friendly processes, FFF has gained increased popularity among the research community. The Acrylonitrile Butadiene Styrene (ABS) is one of the most frequently used polymers in industry. In specific, it is used for the production of automotive parts, protective gear, toys, small appliances components, as well as enclosures for electrical and electronic assemblies.

Samykanou et al. [1] presented a work on the mechanical properties' evaluation in terms of three printing parameters on the ABS polymer. Moreover, the authors have investigated their effect on the studied properties by utilizing a Design of Experiments (DOE) and statistical methods. Similarly, Ouhsti et al. [2] worked on the Poly(lactic Acid) (PLA) plastic by employing the Central Composite Design (CCD) to plan the experiments with three factors. An investigation was made to assess the parameters influence on typical mechanical properties of the PLA, as well as an empirical modeling process was performed. Moradi et al. [3] employed the Response Surface Methodology (RSM) to evaluate three printing parameters during the FFF of an upgraded version of ABS. The study focused on the development of a statistical model for typical outputs such as the tensile strength and the fracture strain. Another study with similar features is the one by Shafahat [4], which studied the tensile testing of PLA under three printing parameters, in addition to the strain rate. The Taguchi method was selected to plan the experiments and the desirability index was used for the characterization of the mechanical properties such as the yield strength, toughness and elastic modulus. Studies that relate to other 3D-printed materials such as carbon-fibre [5] and Acrylonitrile Styrene Acrylate (ASA) [6], as well as different testing methods such as bending [7] and impact [8], rely on similar research methodologies and investigation tools [9,10].

It is evident that several studies in the past few years, focus on the investigation of three parameters with respect to typical mechanical characteristics such as the tensile strength and the strain, by utilizing statistical tools. In the light of the above, this paper investigates the effects of four structural 3D-printing parameters on the Strength-to-Mass ratio (StMr) of ABS polymer. The StMr is a feature with increased impact on the structural efficiency of a specimen that has not been sufficiently studied. The layer thickness (LT), the infill density (FD), the top/bottom layer line direction (LD) and the infill pattern (FP), constitute the key characteristics for the structural integrity of a 3D-printed structure. Furthermore, a shallow ANN model was developed to approximate the specific characteristic under the studied range of conditions.

2. MATERIALS AND METHODS

2.1. Study workflow

The workflow of the present study is illustrated in Figure 1 and is based on the work by Tzotzis et al. [11]. It includes five steps as follows: the design of experiments according to the Central Composite Design (CCD), which yielded thirty-one tests. The specimen fabrication required for the tensile testing. The mass measuring of the fabricated specimens. The realization of the tensile experiments and finally the extraction of the output data and the neural network modeling. All sets of specimens used in the study (two sets of thirty-one parts each) were manufactured with CreatBot D600 Pro printer (Henan Creatbot Technology Limited, Zhengzhou City, China). Ultimaker Cura 4.20 slicing software (Ultimaker B.V., Geldermalsen, Netherlands) was used for the CAD model preparation. Furthermore, Table 1 presents the four printing parameters and their levels.

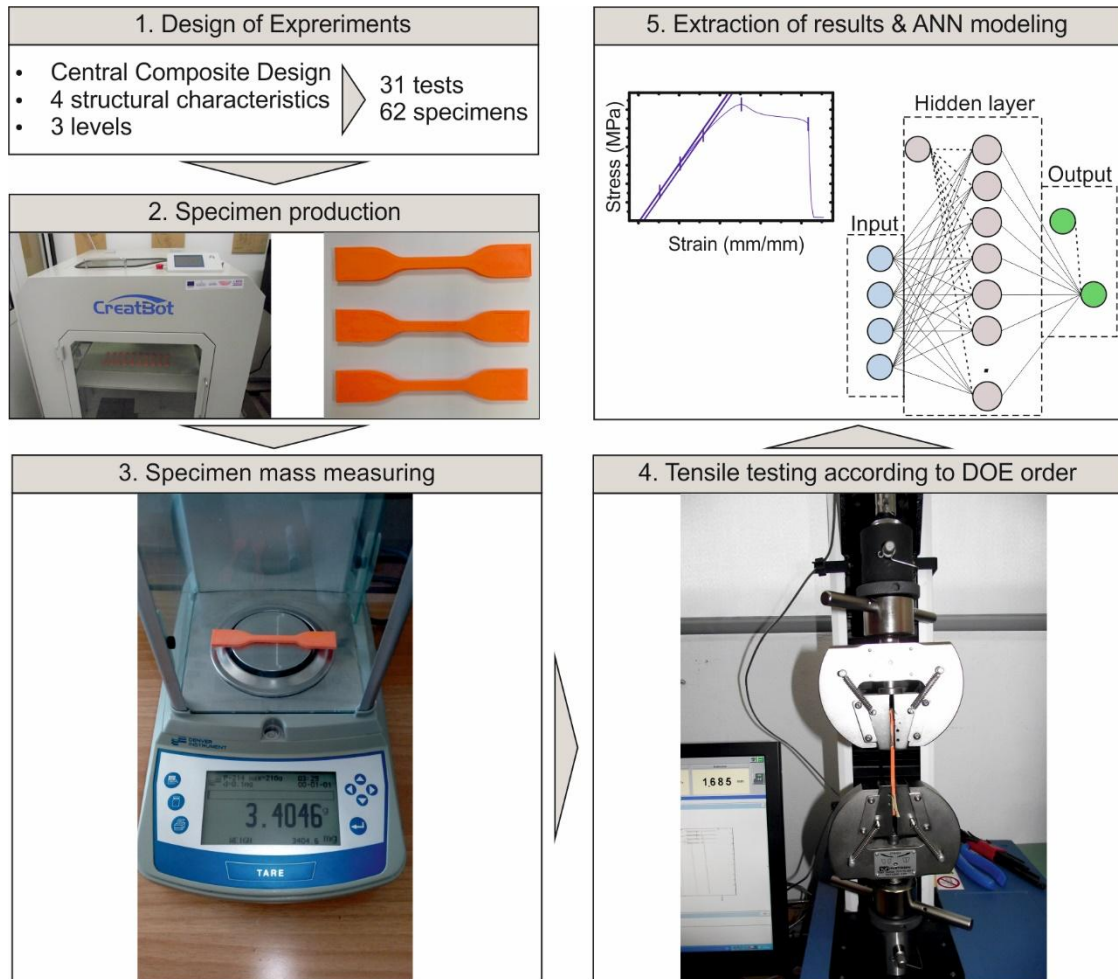


Fig. 1. The study workflow

Table 1. The fabrication parameters and the corresponding levels

Level	LT (mm)	FD (%)	LD (°)	FP
+1	0.3	80	90	Honeycomb
0	0.2	50	45	Triangles
-1	0.1	20	0	Grid

2.2. ANN modeling

To approximate the behaviour of the ABS polymer during tensile loading, ANN modelling was employed. A typical network comprises an input layer, at least one hidden layer and an output layer. Implementation of such networks in manufacturing-related studies is evident in the literature over the past years [12, 13]. This fact is based on the benefits of this method, which can be summarized to the excellent process modelling and pattern recognition. Since the process modelling is the subject of the present study, the development of a shallow network was preferred over more complicated networks.

The network was set according to the feedforward, backpropagation method for the minimization of the difference

between the actual and the net output values. For this purpose, the Damped Least Squares algorithm was utilized, based on the work by Levenberg-Marquardt [14]. The experimental data set was divided randomly, by employing the algorithm “dividerand” found in Matlab™, into three groups: one for training, one for validating and one for testing the developed network. 70% of the total data was used for the training of the model, 15% for the validation and another 15% for the testing.

Table 2 shows the trials performed to identify the ideal network structure for the presented problem. Several shallow structures were tested, and the generated correlation coefficient R were compared, aiming for the highest value. To avoid testing an excess of networks, the minimum and maximum number of neurons were set at 6 and 12 respectively, according to the documentation of Matlab™ [15] regarding underfitting and overfitting. Achieving a high R -value alone does not ensure a good modeling process. As discussed later, other parameters contribute to the robustness of the network as well. Before proceeding however, a high R -value is imperative since it conduces to the best possible degree of the polynomials, limiting both low variance and high bias. In the present study, all structures yielded high R -values, however, the network with six nodes generated the best R -value. Therefore, the 4-6-1 structure was selected for the StMr, comprising four input variables, six neurons in the hidden layer, and one output. Figure 2 illustrates the network structure with the three layers, used in the study.

Table 2. The network structure trials and the equivalent coefficients

ANN structure	R -value
4-6-1	0.99335
4-7-1	0.98195
4-8-1	0.93415
4-9-1	0.96663
4-10-1	0.96532
4-11-1	0.93841
4-12-1	0.96964

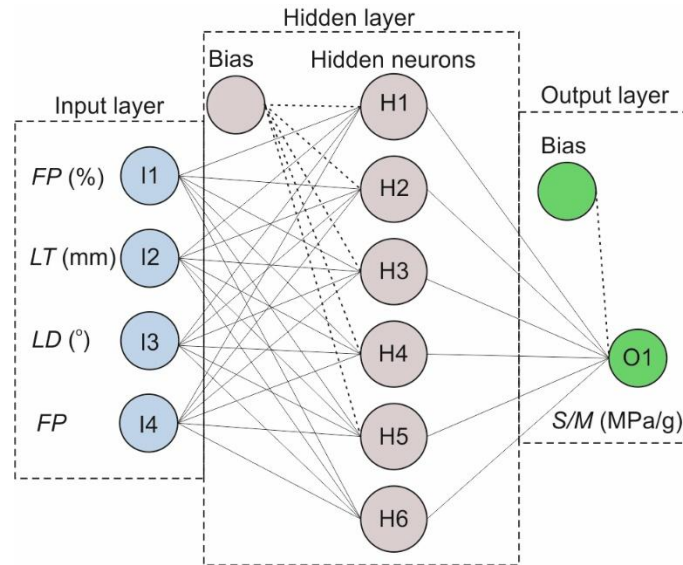


Fig. 2. The selected ANN structure

To match the range $[-1, 1]$ of the hyperbolic-tangent activation function, all data (input and output) were normalized [16]. Equation 1 can be used to estimate the normalized values $y_{normalized}$, with respect to the parameter value y , the y_{max} and the y_{min} , which represent the maximum and the minimum actual value of the input variable or output values respectively.

$$y_{normalized} = \frac{2}{y_{max} - y_{min}} \times y - \frac{y_{max} + y_{min}}{y_{max} - y_{min}} \quad (1)$$

Equation 2 represents the formula that was generated through the shallow network development and can be used to predict the StMr values. Each hidden neuron H_i can be computed with Equations 3 to 8, which have been produced by considering both the weights of the input layer and the biases of the hidden layer, with respect to the activation function.

$$StMr = -0.15824H_1 + 2.0221H_2 - 0.40088H_3 - 0.40813H_4 + 0.75021H_5 - 0.68301H_6 + 0.45463 \quad (2)$$

$$H_1 = \tanh(0.5 \times (0.55177LT - 0.70739FD + 0.98703LD + 1.7412FP - 2.1698)) \quad (3)$$

$$H_2 = \tanh(0.5 \times (1.4258LT - 1.1039FD - 0.86482LD + 0.69072FP - 3.123)) \quad (4)$$

$$H_3 = \tanh(0.5 \times (-0.86211LT - 0.47882FD + 2.8155LD + 0.86575FP + 0.57798)) \quad (5)$$

$$H_4 = \tanh(0.5 \times (-0.094107LT + 1.3077FD - 2.3888LD - 1.2052FP + 0.46211)) \quad (6)$$

$$H_5 = \tanh(0.5 \times (1.3481LT - 0.47891FD - 0.63141LD + 0.83293FP + 2.8577)) \quad (7)$$

$$H_6 = \tanh(0.5 \times (-2.384LT + 0.10976FD + 2.5337LD + 0.043687FP - 2.0413)) \quad (8)$$

2.3. Network evaluation

Figure 3 illustrates the regression plots for the predicted StMr. The plots correspond to the training data set, the validation data set, the training data set and the total data set accordingly. Two characteristics that are identifiable in the plots indicate the strong fit between the experimental and the predicted values of StMr. The first one regard the predicted data points, which are close to the zero-error line ($Y = T$). The second one regard the collinearity between the fit line and the error line. The high R -values generated for all data sets prove the increased accuracy of the model, fact that contributes to the generation of low error rates. More specifically, the coefficient values for the training data set, the validation, the testing and the total of the data points, were estimated equal to 0.99355, 0.98913, 0.99852 and 0.99335 respectively.

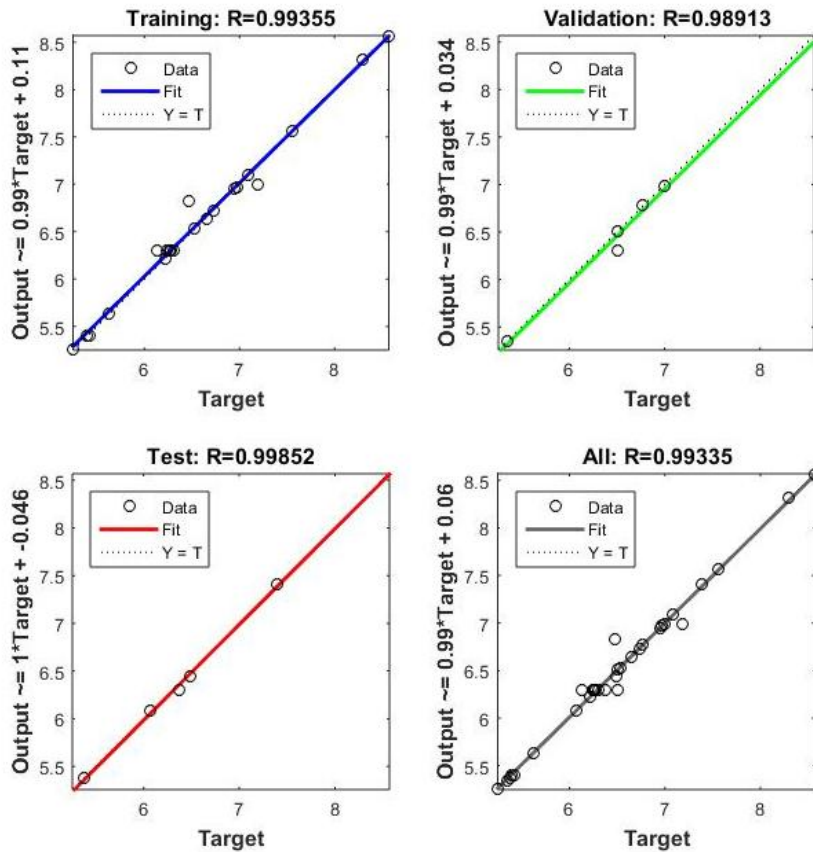


Fig. 3. The regression plots for the training set, the validation set, the test set and the total of the data sets respectively

3. RESULTS AND DISCUSSION

The level means for the four printing parameters were investigated with the main effect plot of Figure 4. It was found that the thicker layer used, the higher the generated StMr. A considerable increase is noticeable at the 0.3 mm value. The infill density at 50% and 80% produces StMr of approximately the same level. In contrast, the lowest level of FD affects positively the yielded ratios, probably due to the notable drop in mass. The 0° orientation

of the top/bottom layers is responsible for the generation of the highest StMr. The following orientations act decreasingly. Similar findings were reported by studies [2,12] that support the fact that both the FD and the LT have a strong impact on the mechanical properties of ABS polymer. Lastly, each of the three patterns applied to the specimens, exhibited a different effect. That is, the triangular pattern contributed the least to the generated tensile strength and therefore to the StMr as well. The grid pattern performed better compared to the triangles. Finally, the honeycomb pattern exceeded both triangles and grid in terms of StMr performance. Furthermore, it is shown that the LT and the LD are the parameters with the most significant contribution.

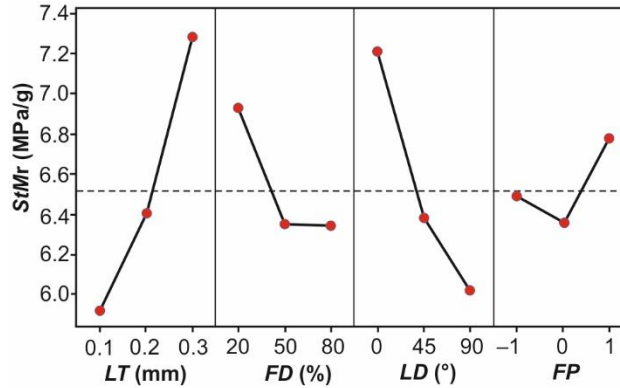


Fig. 4. The main effect plot of the StMr

To evaluate the prediction capacity of the ANN model, a comparison between the predicted and the experimental values for StMr was performed. Figure 5 illustrates the comparison between the StMr datasets. It should be noted that the maximum absolute error was estimated to be 5.5%, while the Mean Absolute Percentage Error (MAPE) approximately equal to 1%, proving the robustness and accuracy of the developed network.

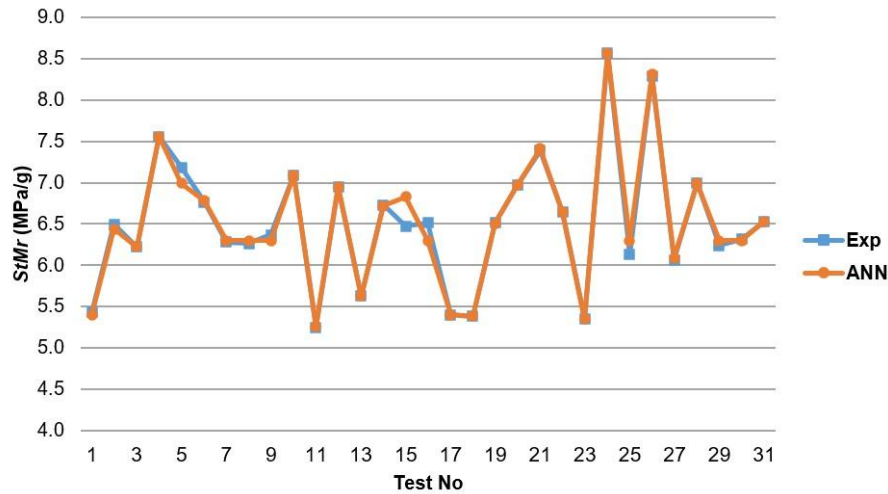


Fig. 5. The comparison between the predicted and the experimental values.

4. CONCLUSIONS

In the present work, two sets of tensile experiments were conducted according to the CCD, involving the ABS specimens fabricated via 3D-printing. The influence of four structural parameters was examined and a shallow ANN was developed for the prediction of the StMr. The fill density, the layer height, the top/bottom layer line direction and the fill pattern were the parameters studied for the specimen performance assessment. In general, it was found that the layer height and the line direction affect the most the StMr, followed by the infill.

Lastly, the next conclusions were derived:

The layer thickness is the most influencing factor, acting increasingly on the generated StMr.

Direction of fracturing is a feature affected directly by the line direction. Consequently, the 0° is responsible for higher StMr values, with the 45° and 90° direction following.

The influence patterns produced by the density, indicate that both the 50% and 80% have almost the same influence. Contrarily, the 20% density contributes towards the achievement of higher StMr values.

Regarding the pattern, the honeycomb was determined to be the one yielding the highest possible StMr compared to the other two.

Finalizing, the ANN model generated predictions of increased accuracy, with the error handling being at the magnitude of 1%.

Funding: This paper has received no external funding.

Conflicts of Interest: There is no conflict of interest.

REFERENCES

1. Samykano, M.; Selvamani, S.K.; Kadirgama, K.; Ngui, W.K.; Kanagaraj, G.; Sudhakar, K. (2019), *Mechanical Property of FDM Printed ABS: Influence of Printing Parameters*. Int. J. Adv. Manuf. Technol., 102, 2779–2796, doi:10.1007/s00170-019-03313-0.
2. Ouhsti, M.; El Haddadi, B.; Belhouideg, S. (2018), *Effect of Printing Parameters on the Mechanical Properties of Parts Fabricated with Open-Source 3D Printers in PLA by Fused Deposition Modeling*. Mech. Mech. Eng., 22, 895–907, doi:10.2478/mme-2018-0070.
3. Moradi, M.; Hashemi, R.; Kasaeian, M. (2023), *Experimental Investigation of Parameters in Fused Filament Fabrication 3D Printing Process of ABS plus Using Response Surface Methodology*. Int. J. Adv. Manuf. Technol., doi:10.1007/s00170-023-11468-0.
4. Ali, S.; Abdallah, S.; Devjani, D.H.; John, J.S.; Samad, W.A.; Pervaiz, S. (2023), *Effect of Build Parameters and Strain Rate on Mechanical Properties of 3D Printed PLA Using DIC and Desirability Function Analysis*. Rapid Prototyp. J., 29, 92–111, doi:10.1108/RPJ-11-2021-0301.
5. Dou, H.; Cheng, Y.; Ye, W.; Zhang, D.; Li, J.; Miao, Z.; Rudykh, S. (2020), *Effect of Process Parameters on Tensile Mechanical Properties of 3D Printing Continuous Carbon Fiber-Reinforced PLA Composites*. Materials (Basel), 13, 3850, doi:10.3390/ma13173850.
6. Sanford, L.T.; Jaafar, I.H.; Seibi, A.; Gohn, A. (2022), *The Effect of Infill Angle, Build Orientation, and Void Fraction on the Tensile Strength and Fracture of 3D Printed ASA via Fused Filament Fabrication*. Manuf. Lett., 33, 569–573, doi:10.1016/j.mfglet.2022.07.070.
7. Dhinesh, S.K.; Arun, P.S.; Senthil, K.K.L.; Megalingam, A. (2021), *Study on Flexural and Tensile Behavior of PLA, ABS and PLA-ABS Materials*. Mater. Today Proc., 45, 1175–1180, doi:https://doi.org/10.1016/j.matpr.2020.03.546.
8. Atakok, G.; Kam, M.; Koc, H.B. Tensile, (2022), *Three-Point Bending and Impact Strength of 3D Printed Parts Using PLA and Recycled PLA Filaments: A Statistical Investigation*. J. Mater. Res. Technol., 18, 1542–1554, doi:10.1016/j.jmrt.2022.03.013.
9. Mazurchevici, A.D.; Carausu, C.; Ciofu, C.; Popa, R.; Mazurchevici, S.N.; Nedelcu, D. (2019), *Infill and Type Influence on Tensile Strength of PLA Biodegradable Material Using FDM Technology*. Int. J. Mod. Manuf. Technol., 11, 44–49.
10. Fadhil Abbas, T.; Basil Ali, H.; Kadhim Mansor, K. (2022), *Influence of Fdm Process Variables' on Tensile Strength, Weight, and Actual Printing Time When Using Abs Filament*. Int. J. Mod. Manuf. Technol., 14, 7–13, doi:10.54684/ijmmt.2022.14.1.7.
11. Tzotzis, A.; Manavis, A.; Efkolidis, N. (2024), *Analysis of the Influence of Structural Characteristics on the Tensile Properties of Fused Filament Fabricated ABS Polymer Using Central Composite Design*. Appl. Mech., 5, 20–35.
12. Alafaghani, A.; Ablat, M.A.; Abedi, H.; Qattawi, A. (2021), *Modeling the Influence of Fused Filament Fabrication Processing Parameters on the Mechanical Properties of ABS Parts*. J. Manuf. Process., 71, 711–723, doi:10.1016/j.jmapro.2021.09.057.
13. Deb, S.; Parra-Castillo, J.R.; Ghosh, K. (2011), *An Integrated and Intelligent Computer-Aided Process Planning Methodology for Machined Rotationally Symmetrical Parts*. Int. J. Adv. Manuf. Syst., 13, 1–26.
14. Marquardt, D.W. (1963), *An Algorithm for Least-Squares Estimation of Nonlinear Parameters*. J. Soc. Ind. Appl. Math., 11, 431–441, doi:10.1137/0111030.
15. Mathworks Matlab, (2023), available at https://www.google.com/search?q=Mathworks+Matlab+2023&rlz=1C1OKWM_enRO931RO931&oq=Mathworks+Matlab+2023&aqs=chrome..69i57j0i19i512j0i19i22i30j0i751j0i512i546l2j0i751j0i512i546.558j0j15&sourceid=chrome&ie=UTF-8, accessed 05.04.2024.
16. Tzotzis, A.; Korlos, A.; Verma, R.K.; Kyratsis, P. (2023), *ANN-based surface roughness modelling of aa7075-t6 slot milling : Cutting technique evaluation*. Acad. J. Manuf. Eng., 21, 27–35.

Received: April 15th, 2024 / Accepted: December 15th, 2024 / Paper available online: December 20, 2024 © International Journal of Modern Manufacturing Technologies.